Mars Ascent Vehicle
Solid Propulsion Configuration

Darius Yaghoubi
Mail Stop EV41
4600 Rideout Road
Marshall Space Flight Center, AL 35812
darius.f.yaghoubi@nasa.gov

Andrew Schnell
Mail Stop ED04
4221 Rideout Road
Marshall Space Flight Center, AL 35812
andrew.schnell@nasa.gov

As part of a Mars Sample Return (MSR) campaign, two Mars Ascent Vehicle (MAV) configurations have been designed in parallel. Each ascent vehicle configuration has a different propulsion system, which ultimately leads to two unique vehicle designs. As part of a Preliminary Architecture Assessment (PAA), these vehicle designs were developed to the same level of maturity in order to inform the selection of one of the vehicles as the point of departure design for the campaign. The selection will be made in November 2019.

Although the initial MSR architecture called for a hybrid-based propulsion MAV featuring solid wax fuel with liquid oxidizer, a configuration using more traditional solid propulsion was developed as an additional risk mitigation option. Though lacking in the single stage to orbit (SSTO) and throttle flexibility of a hybrid configuration, a solid configuration vehicle allows a simpler design with significantly longer flight heritage and higher Technology Readiness Level (TRL).

This paper describes the design of the solid propulsion configuration. An additional paper will be published describing the design of the hybrid propulsion configuration [1]. The solid propulsion configuration MAV was developed in 2019 by NASA Marshall Space Flight Center (MSFC) in association with NASA Jet Propulsion Laboratory (JPL). It features two stages with a modified STAR-17 motor for the second stage and a traditional electromechanical actuator Thrust Vector Controller (TVC). The vehicle was designed to deliver approximately 0.47kg of Martian geological samples to a circular orbit at Mars of 343km at a 25º inclination.

Although solid motor designs in general are at a relatively high TRL, the integrated vehicle subsystems that operate in conjunction with these propulsion elements do not typically operate in a Martian environment, which in this application can get as cold as -40ºC. The PAA advanced the maturity of these subsystems by performing detailed design and analysis on the vehicle with respect to structures and mechanisms, Guidance/Navigation/Control (GNC) systems, avionics, Reaction Control System (RCS), TVC, thermal environments, and advanced Computational Fluid Dynamics (CFD). This paper will summarize the results of these studies.

TABLE OF CONTENTS

1. INTRODUCTION

The Mars Ascent Vehicle (MAV) concept is a significant component of the larger Mars Sample Return (MSR) campaign. The primary objective of this campaign is to return geological samples from the surface of Mars to Earth. Although a multitude of scientific robots and observation satellites currently exist on Mars, technological limitations prevent these platforms from truly duplicating an actual scientific laboratory that one could find on Earth.

The MSR campaign begins with the Mars 2020 rover, expected to launch from Earth in Summer 2020. Upon arriving on Mars, the M2020 rover will spend the next six years collecting samples of dirt, soil, rocks, and other deposits from the Jezero Crater on the Martian surface. The rover will package these samples in tubes and deposit them for collection at a later date. In 2026, MAV will launch from Earth, stowed upon a Sample Retrieval Lander (SRL). Upon arriving at Mars nine months later, the MAV will remain stowed while a Sample Fetch Rover (SFR) collects the deposited sample tubes. The SFR will then insert the sample tubes into the Orbiting Sample (OS), which is the payload for the MAV. After the SFR has completed delivery of 30 sample tubes to the MAV, the MAV will launch from the Martian surface. Upon achieving orbit, the MAV will eject the OS, which will then be captured by the Earth Return Orbiter (ERO) and returned to Earth.

Although a hybrid-based propulsion architecture was originally proposed for MAV, a solid propulsion option was also developed as an alternative. While not as versatile as hybrid motors, traditional Solid Rocket Motors provide their own set of advantages and disadvantages. Perhaps the greatest advantage of SRMs is the relatively high Technology Readiness Level (TRL). SRMs have been used in both manned and unmanned launch vehicles for decades. Additionally, they lack the complexity of liquid and hybrid counterparts. In the solid MAV design, traditional ignition and Thrust Vector Control (TVC) systems were used to add to the TRL. The downside to SRMs however, primarily lie in relative performance. SRMs are unable to be actively throttled or shut down. Additionally, SRMs in general have a lower specific impulse (Isp) than liquid or hybrid motors. Finally, solid motors can potentially encounter internal structural problems when stored at extremely low temperatures, as one would expect on the Martian surface.

Ultimately, a Preliminary Architecture Assessment (PAA) was completed to advance the fidelity of both a solid and hybrid configuration MAV to the same level of maturity. The solid configuration was designed to deliver 30 sample tubes to a circular orbit of 343km at 25º inclination around Mars. While doing so, it had to physically fit and remain operational within the SRL for the duration of the mission, while remaining within a specific mass constraint. The final design for the solid configuration MAV is shown below in Figure 1.

2. PRELIMINARY ARCHITECTURE ASSESSMENT

A PAA was completed to support the MSR campaign by maturing designs for two MAV concepts: a hybrid and a solid configuration, so that managers could make an informed decision on how to proceed with the mission. This paper will describe the solid configuration. In addition to technical design and analysis, the PAA existed to identify potential design issues for each configuration as well as programmatic design issues regardless of configuration. The PAA was the first actual design phase of the MAV.

The solid configuration vehicle began with an initial design phase. This involved an iterative process between GNC (Guidance, Navigation, and Control) and propulsion teams to design a 1st and 2nd stage solid motor combination that would deliver the vehicle to a target circular orbit of 343km along a 3DOF (Degree of Freedom) trajectory. Following the 3DOF analysis, an initial CAD (Computer Aided Design) model was developed, which fed an aerodynamics and mass properties analysis. The results of these were then fed into a 6DOF analysis, ultimately leading to a final design featuring an active TVC (Thrust Vector Control) and RCS (Reaction Control System). Throughout this process, avionics and thermal subsystems were also assessed. Each of these subsystems provided estimated performance values that came into play with the driving requirements of the overall vehicle.

Although the PAA had a number of ground rules and assumptions associated with each of the individual subsystems, the driving guidelines behind the mission itself were comprised of three important factors: orbit quality, physical size, and overall mass. A target orbit of 343km was desired, however, an absolute lower bound of 300km and a "soft" upper bound of 375km with a 25º inclination was needed to interface with the ERO. In addition, an eccentricity of less than 0.006 and a semi-major axis of ±9km was also within the design parameters. For physical size, a maximum length of 2.8m and a maximum diameter of 0.57m was needed to fit within the SRL. The target Gross Liftoff Mass

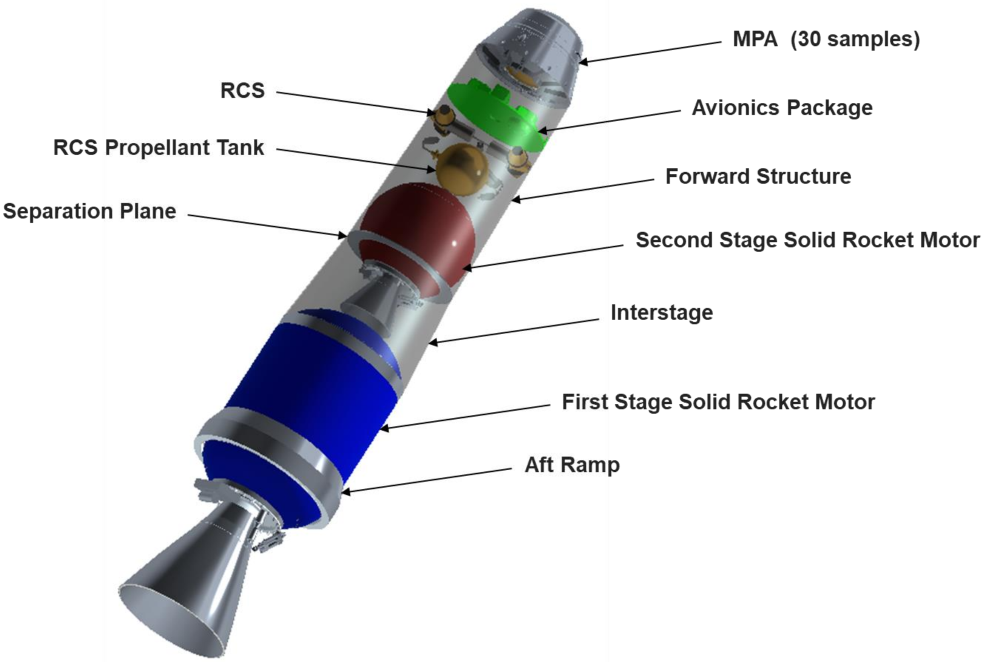

Figure 1. MAV-Solid Configuration Component Layout

(GLOM) was 400kg. The ultimate mission of the solid MAV configuration was to deliver a 16kg payload of 30 tubes of Martian sample to orbit.

3. THERMAL

The thermal environments encountered by the MAV were primarily broken up into two distinct configurations: a stowed configuration, which accounts for transit between Earth and Mars as well as Martian surface operations, and an operational configuration, in which it is actively exposed to the Martian atmosphere. While stowed aboard the SRL, the MAV is stored in a thermal enclosure known as the igloo. The igloo provides thermal insulation for the MAV as well as additional environmental protection from both deep space during transit and the Martian environment while on the surface. Figure 2 shows the MAV stored within the igloo inside the SRL.

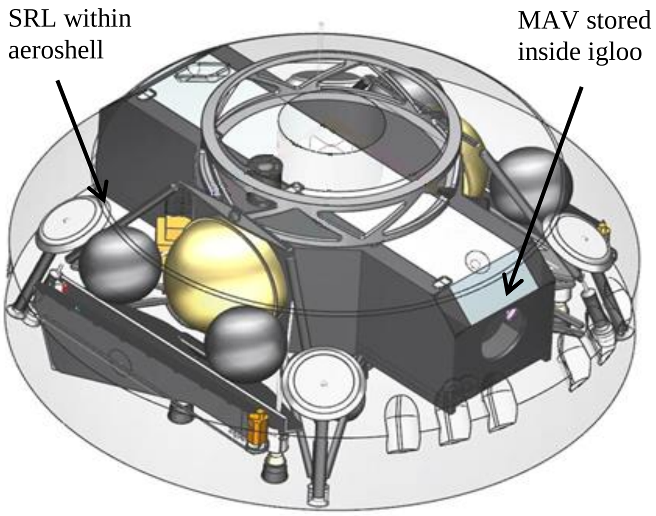

Figure 2. MAV Stowed on SRL

During transit, the thermal environment is driven by the SRL aeroshell temperature and optical properties. While stowed on the Martian surface, the thermal environment is driven by an expected outside temperature boundary of -62.5°C. High Technology Readiness Level (TRL) Thermal Control System (TCS) components are used to maintain MAV operating and non-operating temperatures during these times, as well as during all stages of flight. The primary TCS consists of a series of heaters/sensors, Multi-Layer Insulation (MLI), low emissivity tapes, CO2 gap insulation, and a traditional foam/cork Thermal Protection System (TPS). Although outside temperatures are expected to drop as low as -62.5°C, the TCS is designed to maintain a non-operational Allowable Flight Temperature (AFT) aboard the MAV of -40°C and an operational AFT of -20°C. Some components of the vehicle, such as the Reaction Control System (RCS) will require a different AFT.

The MAV TCS will utilize the same heaters to meet both operational and non-operational AFTs. Platinum Resistance Thermometers (PRTs) will be used to monitor the temperature of the MAV and provide feedback to the SRL for heater management. The vehicle will make use of 16 heater control zones, with each zone including a specific number of heaters controlled by an individual PRT. The basic layout of the heater zones are shown in Figure 3. Different heater sizes and shapes will be required to accommodate various components. Wherever possible, heaters will be wired in parallel to form a level of fault tolerance.

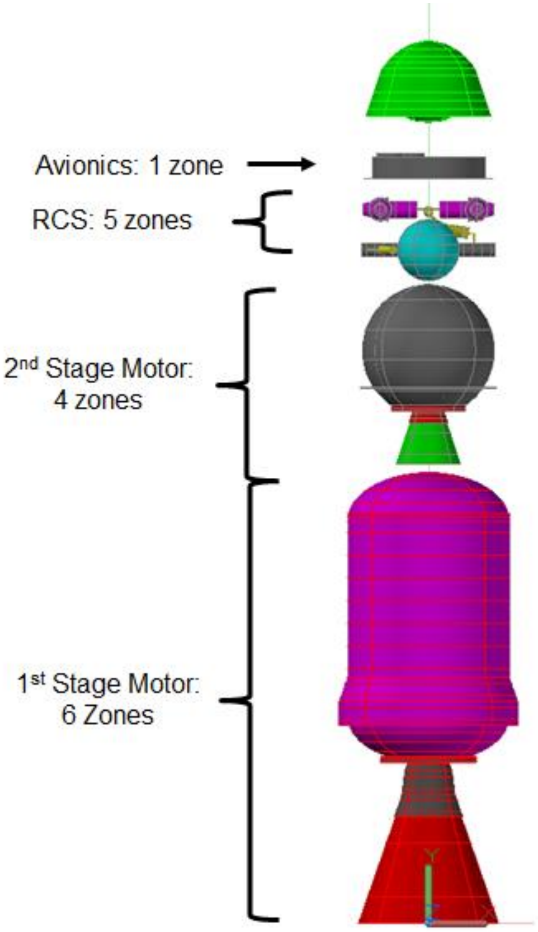

Figure 3. Heater Control Zones

In addition to heaters and sensors for temperature regulation, the MAV design features a number insulation materials. Although not yet in the actual MAV thermal design, MLI is reserved in the overall vehicle mass estimate. This insulation can possibly be used on the avionics to RCS interface and between stages. Blanket construction may include sheets of aluminized Kapton, Mylar, Dacron netting, Nomex threads, and polyimide tape. Low emissivity aluminized polyimide tape can be used to cover heater elements and on interior MAV surfaces. Materials such as these are at a high TRL and are currently used on the International Space Station (ISS), Hubble Space Telescope (HST), and Mars Exploration Rover.

The current vehicle design also features a traditional TPS. This system consists of a 0.5cm thick P50 cork covering the base region area to protect against base plume heating. A 0.5cm layer of Spray On Foam Insulation (SOFI) may also be used on the Outer Mold Line (OML) of the first stage motor to protect from aeroheating as well as insulating some internal components. These TPS methods have been used on Delta IV, Space Shuttle, and Saturn V launch vehicles.

While stowed on the Martian surface, the volume between the igloo and MAV will be filled with CO2, which will act as an insulator by preventing natural convection. Insulation gaps of both 5cm and 10cm were examined for this study. A thermal analysis of the stowed vehicle within the igloo found that the TCS meets the MAV AFTs for transit to Mars, Martian surface operations, and Mars launch/ascent phases of the mission. To meet AFT constraints during Mars surface operations, the igloo 5cm CO2 gap configuration uses approximately 30% more power than the 10cm gap configuration. This applies to both operational and non-operational temperatures. An analysis of this power usage found that increasing the heater power during warmup from non-operational to operational temperatures can increase MAV internal component temperatures up to 2.5 times faster with a total energy decrease of up to 40%. A higher temperature gradient is not necessarily desirable, however, as some components, such the solid motor, may experience cracking if the rate of temperature change is too drastic. A solid motor temperature gradient of 10ºC/hr was desirable to minimize the risk of this solid motor grain cracking. Further thermal analysis found that at heater powers exceeding 200W, the 10cm CO2 gap configuration exceeded this motor temperature gradient. Ultimately, peak power from the thermal system during warmup was found to be 288W at a voltage of 36VDC.

4. AVIONICS

The MAV avionics system has three primary functions: maintaining command and data handling, communication, and providing power during flight. When possible, high TRL components were used, although a number of custom hardware elements were necessary. The primary hardware components used in the avionics design were an IMU (Inertial Measurement Unit), star tracker, radio transceiver, batteries, power distribution board, input/output board, and flight computer. The layout of the avionics hardware are shown in Figure 4.

Command and data handling is primarily carried out by the flight computer, star tracker, and IMU. These hardware components allow the vehicle to determine its attitude and positional data during flight. They also ensure the correct execution of custom GN&C algorithms through custom flight software. Communications are managed by the transceiver, antenna, and navigational beacon. All communication is with the Mars Relay Network (MRN), which is capable of returning data to Earth.

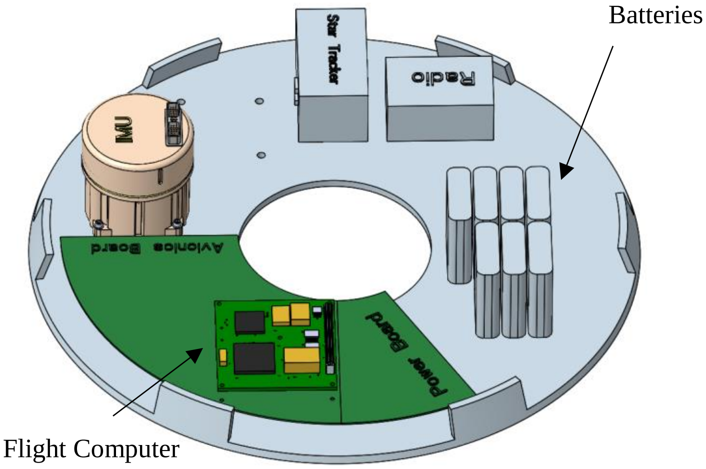

Figure 4. Avionics Hardware Layout

Although the transceiver and antenna are important for broadcasting position and trajectory data, the sole purpose of the beacon is for the ERO to locate and capture the OS. Note that the beacon is not included in the avionics hardware, as its location within the vehicle is still to be determined. A custom distribution board is designed to administer power from an array of batteries to the individual avionics components. These batteries also provide power to the thermal heaters throughout the vehicle. A significant amount of cabling was needed to deliver power to these heaters. The beacon was powered independently. The overall avionics hardware architecture is shown in Figure 5.

Prior to the actual start of the ascent portion of the MAV mission, a number of functions will be provided by the SRL. Attitude and position knowledge will be provided for state initialization and calibration of the IMU. Communications between the MAV and ground operations crew on Earth will be provided via umbilical connection. Fault protection will also be available to detect any off nominal conditions such as environmental or sensor effects found during regular health and safety checks. Additionally, the SRL will provide power to support battery charging and on board heaters. This will ensure that the MAV will only be under its own power for the ascent and orbital insertion portions of its mission.

A Sphinx flight computer was assumed for use as the primary computation component for command and data handling. This computer was developed by NASA JPL and selected based on its mass, power, and radiation tolerance. Although the actual flight software has not yet been developed, a customized version of the Core Flight System (cFS) framework will be used on the Real-Time Executive for Multiprocessor Systems (RTEMS) operating system. The main software functionality will ensure that launch commit criteria are met, confirm launch once it has been commanded, interface with the IMU and star tracker to control RCS and TVC actuators, transmit navigation telemetry to the MRN, identify any error conditions, command/confirm stage separation, and command/confirm OS separation.

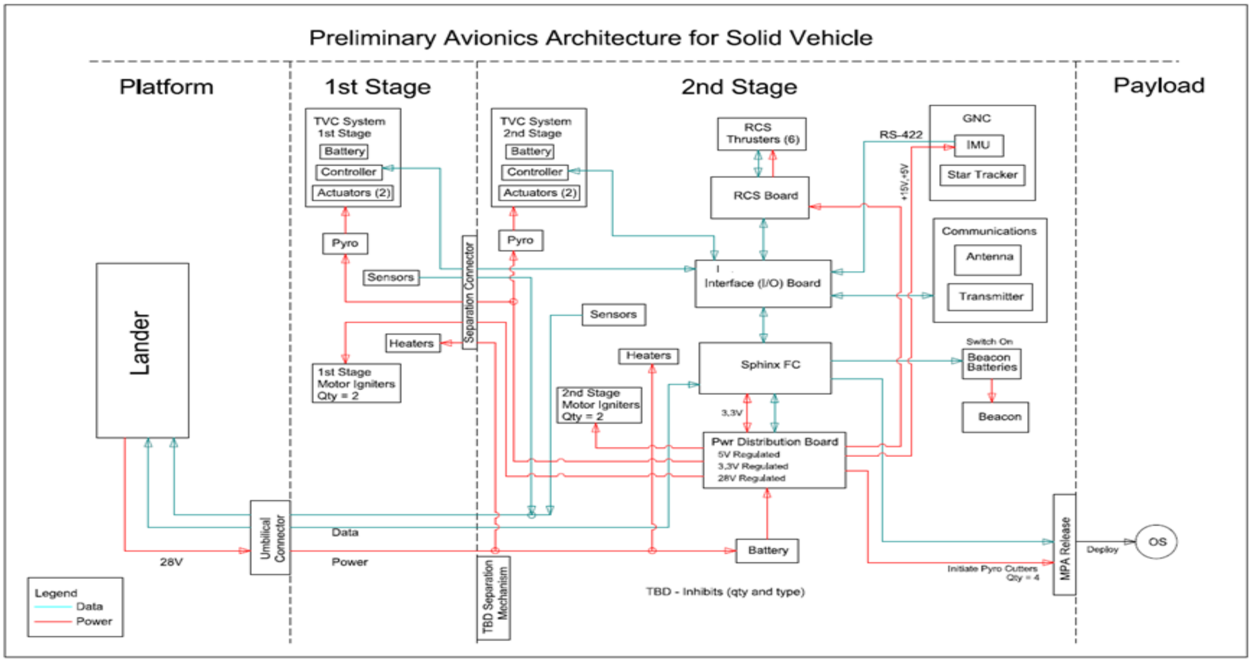

Figure 5. Avionics Hardware Layout

For position and navigational sensing, sensors similar to the Honeywell HG5700 IMU and the Blue Canyon Technologies Nano Star Tracker (NST) were selected. The HG5700 capability was selected due to its small size and navigation-grade performance. This is necessary for achieving accurate attitude knowledge through gyrocompassing. An IMU such as this would still require qualification testing for space environments. Future studies will look at options to reduce vehicle performance requirements, which could potentially result in a smaller IMU. The star tracker can be used to augment the capability of the IMU for further performance. It was baselined for its size, weight, power requirements, and extensive flight heritage. The current GNC design plans to only use the star tracker after leaving the Martian atmosphere. The sizing of these sensors are further detailed in Section 9.

The transmission of critical flight data such as flight phase and telemetry to the MRN was assumed to be provided by a transceiver similar to the ISIS TRXVU. Although this transceiver is capable of both sending and receiving communications, it was only used in this regard in a transmit functionality. The TRXVU was chosen due to its size, capability, and compatibility with the MRN. It will be used in conjunction with either an omnidirectional wraparound or patch antenna. The aforementioned beacon will also use this antenna to broadcast position data to the MRN for capture of the OS by the ERO. This beacon will remain operational on the spent MAV upper stage for up to 45 days following OS orbital injection.

While stowed prior to flight, power will be provided to the MAV by the SRL through an umbilical connection. During flight, however, onboard power will be needed to power avionics components, TCS, RCS valves, and TVC actuators. This power will be provided by batteries similar to SAFT 176065 cells. These cells were selected for their ability to perform in cold temperatures, low loss during long storage periods, and recharge ability.

5. PROPULSION

The solid configuration MAV consists of two stages, each with a modified commercial system SRM. As with typical SRMs, motor burn times and thrust profiles are defined beforehand in the design phase. Burn rate is ultimately tied to pressure, whereas the thrust profile is based upon solid grain shape as it changes surface area over time. As both of these parameters are also affected by propellant temperature, operation in a Martian environment presents a unique condition.

Initial sizing and optimization of the SRMs began with a 3DOF design of experiments. This showed that the initial vehicle and motor design could close with a GLOM less than the driving requirement of 400kg. Additional developments and sizing of the First Stage Motor (SRM1) enabled greater performance through optimization of non-propulsion inert mass, composite case design, and nozzle contouring. The Second Stage Motor (SRM2) utilized a scaled inert geometry from SRM1. Ultimately, SRM1 featured 216kg of propellant, while SRM2 featured 54.4kg of propellant. Although the actual solid motor designs cannot be shown due to International Traffic in Arms Regulations (ITAR), a similar motor design which these designs are based upon, the Northrop Grumman STAR 17 motor [2], is shown in Figure 6.

A trade study was performed to evaluate the suitability of propellants for the MAV mission. Eight individual propellants were examined and compared based upon motor non-operational temperature range, operational temperature range, performance, and heritage.

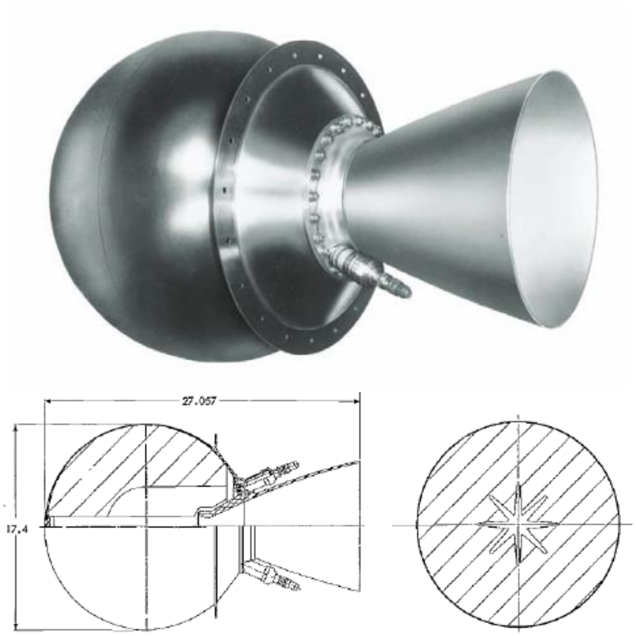

Figure 6. NG Star 17 Solid Rocket Motor

This study found that TP-H-3062 had the most desirable performance for both SRM1 and SRM2. Its Carboxy Terminated Polybutadiene (CTPB) binder allowed a very capable temperature range. Additionally, it has significant heritage, operating in a Martian environment for both Mars Exploration Rovers Spirit and Opportunity and Mars Pathfinder during (Entry-Descent-Landing) EDL. I_{sp} for both SRMs were calculated based upon propellant inputs and nozzle geometry. Although only analytical at this point, static and flight testing will further refine the I_{sp} throughout the MAV design lifecycle.

A structural analysis of the MAV propulsion systems featured a number of load cases for both motor case and propellant loading. These loads were driven by various combinations of Mars surface and launch pressures as well as minimum and maximum expected temperatures. The analysis found that a composite case would appropriately contain propulsion loads in the first stage, with a titanium case for the second stage. A thermal analysis of the motor and nozzle was also completed to determine throat erosion rates and a suitable thickness of insulation.

A Computational Fluid Dynamics (CFD) analysis was performed on the propulsion system to determine a number of induced environments. Plume induced environments for on the SRL were determined at multiple times during MAV launch, including surface pressures and heat fluxes. Both direct and indirect plume interaction were found with the SRL during this time. During SRM1 ignition, high temperature and pressure regions were found in the vicinity of shock fronts near the SRL. Additionally, pressure waves reflected from the Martian surface contributed to the indirect plume impingement. Acoustics, from both an internal chamber perspective and from a liftoff and plume-induced environment perspective were also analyzed. Thrust oscillation analysis found that longitudal modes were unlikely to establish during burn. Liftoff acoustic analysis found the liftoff environment to be benign compared to a similar terrestrial launch arrangement and that ultimately, acoustics during liftoff were not a concern. A similar conclusion was drawn from plume induced acoustic environment and ignition overpressure analyses.

As mass and orbit quality are both driving requirements for the MAV, it was vital that the solid motor design include a fair amount of flexibility. Because of this, it was desired that the propulsion systems allow for offset mass increases of other vehicle subsystems. The designs themselves included a length margin of 10cm on SRM1 and 1.8kg of propellant mass margin in SRM2. This has the added benefit of minimizing Isp uncertainty and providing addional ΔV if needed to adjust trajectory during flight in the event that an energy management maneuver is necessary. Further dispersed analysis on Isp will allow for further optimization beyond the PAA.

6. RCS

The MAV RCS consists of a hydrazine blowdown system containing high TRL components. A nitrogen cold gas system was originally considered, but ultimately disallowed due to its relatively low Isp, which would require an unreasonable amount of propellant mass over hydrazine. Aside from the actual propellant tank, which is located directly below the avionics plate, the MAV RCS features six independent thrusters. The overall layout is shown in Figure 7.

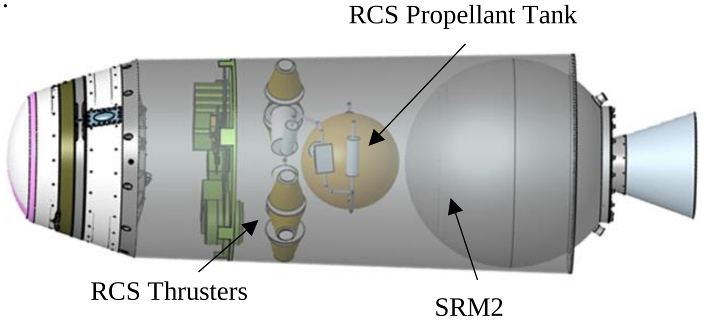

Figure 7. RCS Located on Second Stage

The RCS provides attitude control authority during all phases of MAV ascent. During SRM1 and SRM2 burns, the RCS only provides roll control, as TVC controls pitch and yaw. During the coast period, however, roll, pitch, and yaw are all controlled by RCS.

The thrusters used for RCS are arranged in two groups of three. Ideally, the thrusters would be arranged in a module similar to what is shown in Figure 8, as individual thrusters will be difficult to mount into tight spaces.

The RCS propellant is stored in an aluminum alloy diaphragm tank. The metal diaphragm allows for a reduction in ullage within the tank, thereby minimized RCS slosh.

Gaseous nitrogen is used as the pressurant, pushing the liquid hydrazine out of the top of the tank. One thing of note with hydrazine is the relatively high freezing point of 2°C. As this is significantly higher than the expected non-operating temperature of -40°C, a significant amount of heaters are necessary.

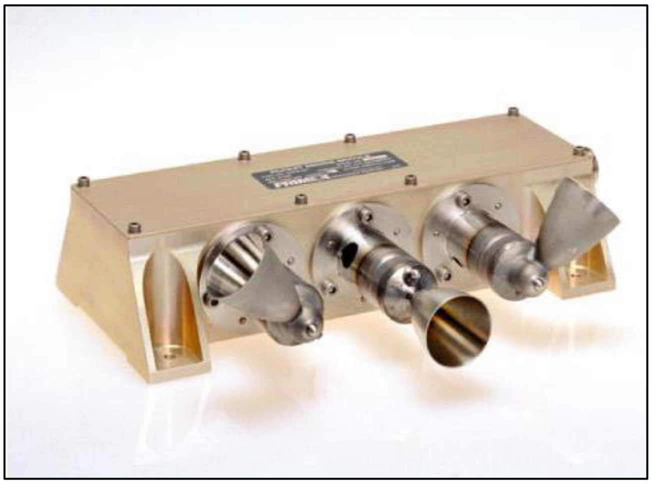

Figure 8. Sample RCS Thruster Module

7. TVC

High TRL TVC system components are used to actuate the MAV supersonic split line gimballed nozzles. A supersonic split line nozzle is a trapped ball design that allows for vectored thrust. The actual joint of the nozzle is located downstream of the nozzle throat, meaning it is removed from the high pressure combustion environment, theoretically reducing erosion. The MAV TVC is present on both stages of the vehicle, and controls pitch and yaw during all stages of flight featuring a motor burn. Gimballing is performed through the use of two traditional electromechanical actuators located on the aft end of each stage. Additionally, thermal batteries and actuator feedback sensors are incorporated. The sensors themselves provide data such as nozzle position, exit velocity, load, and motor temperature to the onboard flight computer. The exact location of the TVC components are shown in Figure 9.

The TVC performance was driven by a maximum gimbal angle of 5°. This was determined through a motor ignition and gimbal angle sensitivity study relating angle and nozzle side loads. The supersonic split line nozzle was a solution with heritage experience that was chosen in an attempt to eliminate elastomeric materials that are known to be incompatible with Martian environmental conditions.

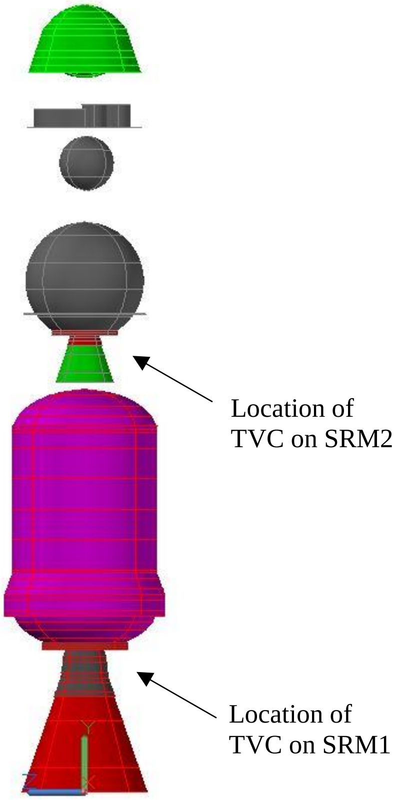

Figure 9. TVC Locations

This does, however, introduce a risk to TVC development in general, as there is an overall lack of experience with such a TVC system at such low temperatures, including performance of supersonic split line nozzles and electromechanical actuators. The actual actuators themselves are similar to what can be found on a Northrop Grumman STAR 12GV solid rocket motor [2], shown in Figure 10.

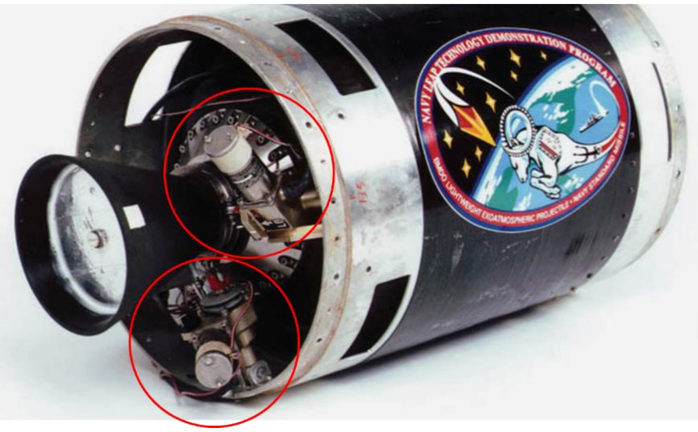

Figure 10. NG STAR 12GV TVC Actuators

8. STRUCTURES

A structural analysis was performed on the integrated vehicle to ensure that it would survive the loads environments encountered during its mission. A typical launch vehicle undergoes maximum load in an axial direction during ascent. MAV presents a unique situation, however, as it is expected to experience a maximum acceleration of approximately 15g in a lateral direction while stored on the SRL during Martian EDL. Additionally, the initial Center of Gravity (CG) of the vehicle plays an important role in this regard, as the overall balance and performance of the SRL is effected by MAV CG. MAV was structurally designed to have monocoque construction, therefore making its structural attach hardpoints to the SRL a significant point of design. Integration with SRL designers found that the attach hardpoints would be most effectively located at SRM flanges with the vehicle CG straddled in the middle, therefore avoiding a cantilevered CG. Figure 11 shows the location of the vehicle attach points to the SRL in relation to its initial CG.

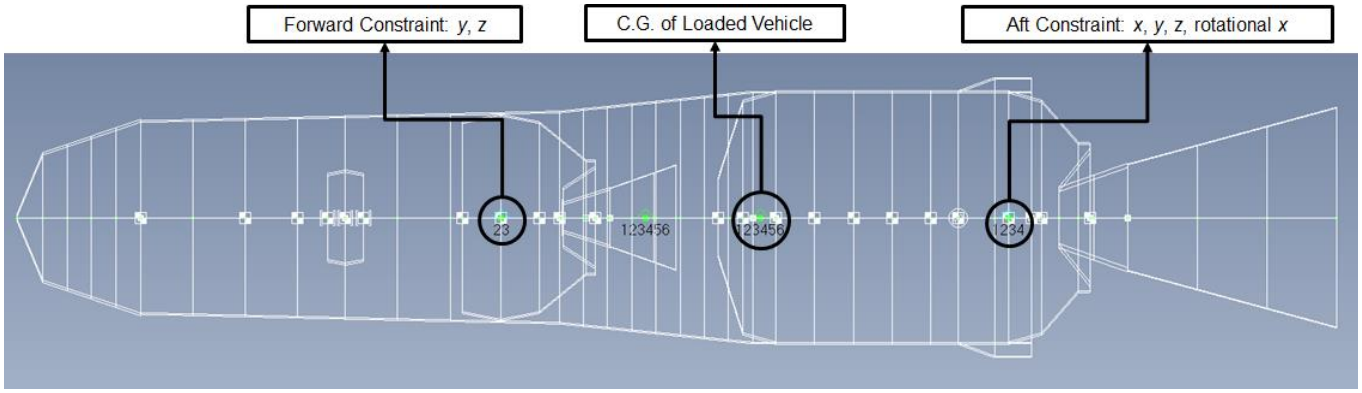

Figure 11. SRL Attach Points

Although the EDL phase was the highest structural loads environment that was found, the analysis also assessed the vehicle response to Earth departure, parachute mortar firing, parachute snatch, and Mars touchdown loads. Integrated vehicle components such as the forward structure, separation system, interstage, and aft ramp were examined. No stiffening elements were designed or included in the design. Assuming an aluminum alloy material type for the second stage forward structure and interstage allowed for the material thickness of these components to be determined. This material thickness calculation took into account failure modes such as strength failure and buckling, and included a yield strength factor of safety of 1.25 as well as an ultimate strength factor of safety of 2.0. The separation system was assumed to be similar to a Planetary Systems Corporation Lightband non-pyrotechnical system. This employs a system of springs to initiate stage separation, and imparts a significant high acceleration load on both itself and the integrated vehicle. Although the MAV separation system mechanism has not been fully expanded upon, this assumption allowed for early mass estimates. Further in depth analysis of additional separation mechanisms will allow for higher fidelity analysis and trade studies. The first stage aft ramp is in place to provide aerodynamic stability and was assumed to take no significant load.

In addition to the aforementioned loads, an induced aeroacoustisc loads environment was developed in order to determine the effects of unsteady aerodynamics on the vehicle. This analysis found that the induced sound energy on the vehicle was encountered at a maximum by the first stage SRM during ascent. Due to the relatively thin Martian atmosphere, this aeroacoustic environment can be compared to the sound energy generated by a simple attached turbulent boundary layer on an aircraft wing traveling at subsonic speeds. Although this would be harmful to a human ear, no significant impact was found from the loads this generated on the vehicle itself. If the skin of the vehicle were to be decreased in thickness at some point in the future, it is possible that the aeroacoustics environment may pose a larger threat. Although buffet loads were originally considered for the PAA, it was later determined that differences in buffet forcing functions between solid and hybrid configurations would be minimal, and therefore development of that analysis was deemed out of scope.

9. GNC

The solid MAV configuration was designed to deliver a 16kg payload to a circular orbit of 343km at a 25^o inclination. An iterative process was necessary to design and analyze a vehicle trajectory capable of completing this mission. Additionally, performance capability of the vehicle RCS and TVC was assessed. In order to determine necessary vehicle parameters, a navigation sensor study was also completed.

Initial mission analysis for MAV featured design of a 3DOF trajectory. Although this type of trajectory only considered translational motion of a point mass, it was vital in determining how the overall vehicle payload mass would factor into the vehicle GLOM as well as overall capability of the two solid motors. Ultimately, the 3DOF trajectory determined the necessary vehicle thrust and propellant flow rates, which were used in sizing of the solid motors. The nominal 3DOF flight plan is shown in Figure 12, featuring an open loop first stage burn to MECO, coast to apoapsis, stage

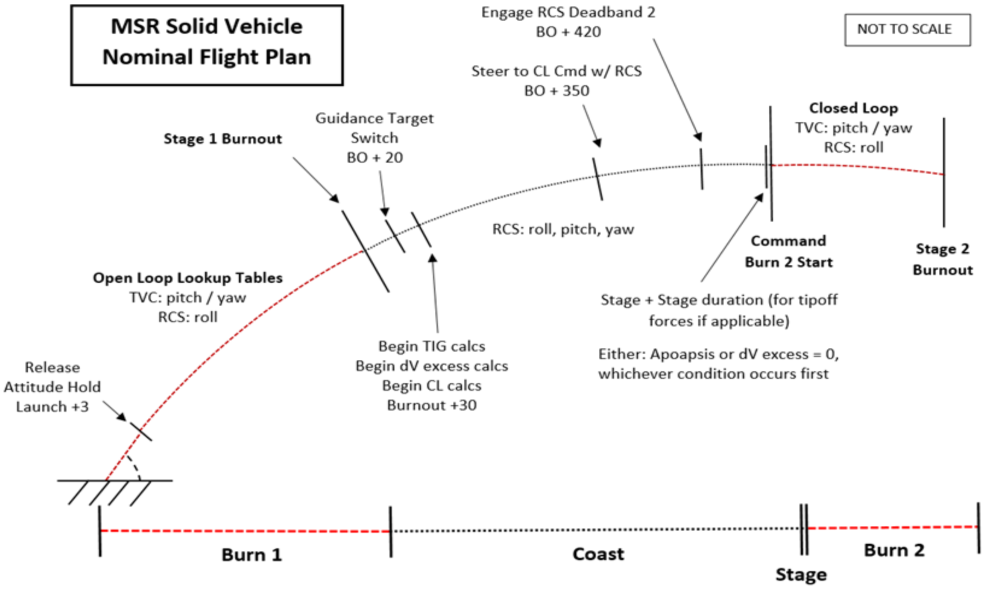

Figure 12. Vehicle 3DOF Flight Plan

separation, and second stage closed loop burn to circularize orbit. Following the design of the 3DOF trajectory, an updated Mass Equipment List (MEL) was generated from other vehicle subsystems and integrated with an aerodynamic database to design a 6DOF trajectory. This trajectory featured vehicle roll, pitch, and yaw rotational body rates in addition to translational motion. The 6DOF analysis was vital in determining how capable the TVC and RCS needed to be, as well as evaluating how well mission design objectives were met. The nominal 6DOF trajectory found that all original design metrics were met with regard to target orbit and GLOM, while remaining within physical size constraints. Of note, it was determined that the CG was aft of the Center of Pressure (CP) during first stage burn, making the vehicle aerodynamically unstable. As shown in Figure 13, this instability was only marginal, with the MAV still being controllable.

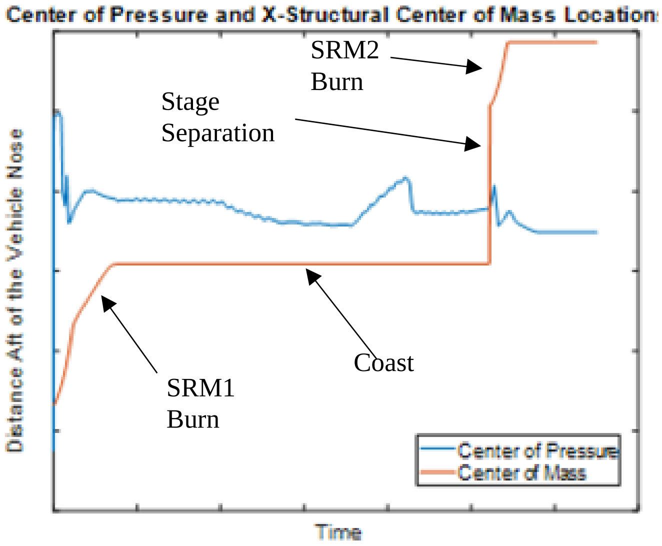

Figure 13. Aerodynamic Stability

In addition to assessing the capability of RCS and TVC needs, the nominal 6DOF trajectory analysis revealed the presence of excess motor energy in the design. During MAV coast phase, one of two events will occur: either the vehicle will reach apoapsis, or the predicted ΔV required to achieve target orbit will match the predicted onboard stage 2 ΔV capability. Whichever of these events occurs first will trigger staging and SRM2 ignition. This second stage burn is performed slightly before predicted apoapsis, expending excess energy by lowering apoapsis while at the same time raising periapsis. Effectively managing this excess energy allows the nominal 6DOF trajectory to close with the target orbit.

A number of simulations with dispersed parameters were performed to determine their effect on the vehicle's performance. Due to the aforementioned excess motor energy issue, the SRM1 Isp was varied to create burnout state variations. By igniting SRM2 according to the vehicle's energy needs, apoapsis cases exceeding the 375km soft upper limit were reduced significantly. Although energy management does address SRM1 Isp variations, it cannot address unknown SRM2 Isp variations. Vehicle mass parameters, motor performance, launch conditions, and atmospheric conditions were varied to determine their effect on key orbit metrics such as altitude, inclination, and eccentricity.

For launch condition dispersions, 100 individual cases were run. These cases specifically varied launch angle and azimuth. All 100 dispersed cases were found to fall within target orbit boxes.

For modeling of the Martian atmosphere, the 6DOF model calls upon a lookup table built from the Mars Global Reference Atmosphere Model (MarsGRAM). To vary environmental conditions, two cases of solar flux and dust tau lookup tables were built. Both cases showed final orbits within the target boxes.

A payload mass knowledge error dispersion was performed to address cases where the vehicle's predicted payload mass was not loaded onto the vehicle. This is especially applicable, as the density of the Martian samples collected will vary. The analysis found 11 failed cases out of 50. These failed cases resulted in the semi-major axis constraint being violated when the mass was either too low or too high.

To assess motor performance, a parametric Isp variation was performed. The Isp for both motors was scaled by the same percentage according to scaling equations developed by solid propulsion subject matter experts. All dispersed cases met minimum periapsis, eccentricity, and inclination target bounds. A number of cases, however, were found to exceed semi-major axis bounds. These failures were primarily driven by SRM2 Isp variations alone, which cannot be detected prior to burn. Holding SRM2 Isp constant while varying SRM1 Isp found no semi-major axis violations. Of the 100 cases ran, 9 exceeded the 375km soft upper limit. Although the majority of these failures were due to a maximum SRM2 Isp variation, some cases were also due to a combination of both stages.

A GNC analysis was performed on the vehicle RCS capability. As mentioned in Section 6, RCS thrusters are used for roll control during first and second stage burns, as well as for roll, pitch, and yaw control during coast. Six RCS thrusters were sized with two to control yaw and four to control pitch and roll. The RCS controller itself was designed as a Proportional-Derivative (PD) controller with on/off thruster command logic. A sensitivity study was performed on both thruster size and placement on the vehicle. This allowed for a nominal thruster size, providing low propellant usage and a suitable attitude response. Additionally, it provided a nominal location for the RCS thruster plane, allowing for an optimal amount of control torque with regard to propellant usage. Dispersed analysis was also performed to determine the amount of RCS propellant consumption necessary with varied vehicle mass properties, aerodynamic coefficients, and thruster Isp. Of the 44 dispersed cases that were run on RCS, a number of cases were found to exceed the semi-major axis constraint when specific off nominal moment of inertia and aerodynamic coefficients were dispersed. Two cases were found to exceed the target orbit altitude soft upper limit when Isp variations were included. Although a maximum required amount of RCS propellant was determined from the performance analysis, it should be noted that there are additional events that were not yet considered that could potentially add to this amount, such as stage separation induced body rates and thruster misalignments. These will be considered in future MAV analysis cycles.

As mentioned in Section 7, TVC is used to provide pitch and yaw control of the motors during burns. As with the RCS, the TVC control algorithm is a PD controller. A GNC performance capability assessment was completed on the TVC design. The maximum TVC gimbal angles were found to primarily be a function of aerodynamic disturbances and internal disturbances such as misalignments and lateral CG offsets. Additionally, duty cycles and maximum TVC gimbal rates were computed for both stages.

A navigation sensor study was performed to select an appropriately capable IMU for the vehicle. Two sensors, a Honeywell HG5700 and a Sensonor STIM300, were compared based upon their physical size, mass, and overall performance. An overview of these sensors with respect to their nominal specifications are shown in Figure 14. Two comparable IMUs are included for reference.

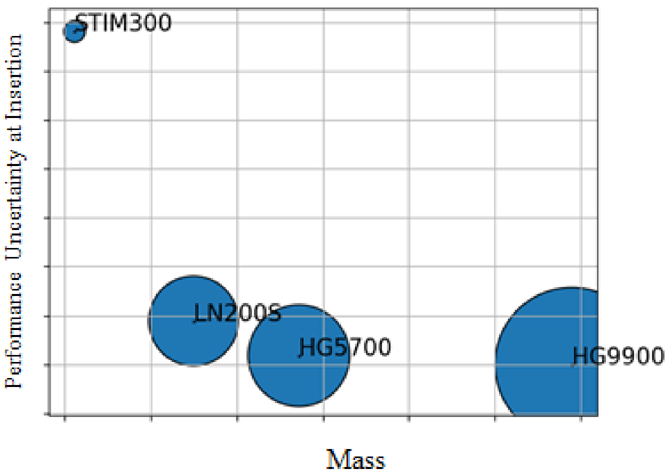

Figure 14. IMU Specifications

Figure 14 shows that as IMU performance capability increases, mass and physical size increase. As all three of these specifications are pertinent to the vehicle design, a Monte Carlo analysis was performed to further determine capability. This used a nominal 6DOF simulation base featuring a variety of errors such as bias, scale factor, internal misalignment, and white noise. Additionally, as mentioned in Section 4, a star tracker was introduced to the navigation system to further augment the IMU capability as needed. The system in general is highly sensitive to initial attitude knowledge.

The Monte Carlo analysis featured 2000 individual simulations for each IMU, both with and without star tracker integration. The simulations featured open loop guidance on the first stage and closed loop guidance on the second stage. Without star tracker integration, the STIM300 IMU was found to only reach the target orbit with 17% of the cases, whereas the HG5700 achieved target orbit with 99.5% of the cases. With the addition of the star tracker, the STIM300 capability increased to 71.3% whereas the HG5700 increased to 99.8%. This showed that the STIM300 was a poor performer in this application, and the vehicle was more suited for the HG5700, or an IMU with similar specifications.

10. SUMMARY

The solid configuration of MAV successfully delivers a 16kg payload of 30 sample tubes to Martian orbit. The mission design constraints for both size and weight were met under nominal conditions. The target orbit was achieved with most 6DOF dispersions, however some cases were found to exceed the design constraint soft limits. Energy management maneuvers can be employed to mitigate these constraint violations. Further studies can expand upon the design of the solid configuration MAV and increase its maturity.

ACKNOWLEDGEMENTS

The authors would like to thank the entire MAV team for their hard work and contributions to the PAA.

REFERENCES

[1] Mars Ascent Vehicle Hybrid Propulsion Configuration, IEEE Aerospace Conference, March 2020

[2] Northrop Grumman Propulsion Products Catalog, June 2018. https://www.northropgrumman.com/Capabilities/PropulsionSystems/Documents/NGIS_MotorCatalog.pdf

BIOGRAPHY

***Darius Yaghoubi** received a B.S. in Aerospace Engineering from North Carolina State University in Raleigh, NC in 2007. He has worked at NASA MSFC for 12 years. He has been an active member of the MAV team since February 2018, initially starting as the GNC lead and transitioning to the vehicle technical lead in October 2018. Prior to joining the MAV team, he worked as the lead pogo stability analyst on the NASA SLS program and supported separation and liftoff analysis on the NASA Ares program. He has also supported NASA groups in loads and dynamics, software integration, engineering testing, 3D printing, and deep space habitat. Aside from his technical work, Darius is an active member of the MSFC Speaker's Bureau and has represented NASA at a number of public outreach and speaking events*

***Andrew Schnell** is a study lead and thermal system designer for Marshall Space Flight Center's Advanced Concepts Office. In over six years in Advanced Concepts, he has led ACO's design efforts on a variety of conceptual design studies including the Lynx X-Ray Observatory, Mars sample return missions, the Europa lander de-orbit stage, the HabEX telescope, and SLS's Exploration Upper Stage. He has also contributed thermal designs for deep space habitats, interstellar probes, solar sails, satellites, cubesats, SLS payloads, and ISS experiments. Prior to joining Advanced Concepts, Andrew was a member of NASA's Cryogenic Fluid Management team, where he managed the design and preparation of several cryogenic test articles. He holds a patent for the design of novel foam-rigidized inflatable structures. Andrew is a graduate of Tennessee Technological University.*